TERMINAL VELOCITIES OF ICE CRYSTALS

by

Stanley R. Brown

This report was prepared with support from
the National Science Foundation
Grant No. GA-11574
Principal Investigator, Lewis O. Grant

Department of Atmospheric Science
Colorado State University
Fort Collins, Colorado

December 1970

Atmospheric Science Paper 170

ABSTRACT

A theoretical consideration of the terminal velocities of several ice crystal types is presented. The Best number-Reynolds number relationship for objects whose shapes simulate ice crystals is employed in the computations. The computed terminal velocities as a function of crystal size are shown.

A parallel field study has been performed. Photographs of crystals falling in natural snowfall were made using a strobe light for illumination. From the photographs, a determination of crystal type, size, and falling attitude and the distance the crystal fell between successive strobe flashes was made. Terminal velocities were then calculated and the data was plotted as a function of crystal type and size. Curves were fitted to the data using the least squares method. These results are shown with the computed values. Also shown are Nakaya's findings for comparison.

Experimental results of the study show that all of the crystal types observed exhibit a functional relationship between terminal velocity and crystal size. This is consistent with theoretical predictions developed in the study. Reasons for some disagreement between observational and theoretical results are discussed.

Stanley R. Brown
Department of Atmospheric Science
Colorado State University
Fort Collins, Colorado
November 1970

ACKNOWLEDGEMENTS

The author wishes to express his appreciation to Professor Lewis O. Grant for his helpful suggestions made during this investigation. Thanks are due Drs. M. L. Corrin, Charles Knight, and Takeshi Ohtake for their helpful discussions. Mrs. Joanne Jermier is also thanked for typing this manuscript under a tight time schedule.

This research was sponsered by the National Science Foundation under Contract GA-11574.

TABLE OF CONTENTS

TABLE OF CONTENTS-CONTINUED

LIST OF FIGURES

LIST OF FIGURES-CONTINUED

INTRODUCTION

Over the past decade, Colorado State University has been conducting a program in the central Colorado Rockies to investigate cold orographic clouds, associated precipitation processes, and their modification potential. An inherent part of this program has been the attempt to refine the description of various cloud physics processes. A cloud process which has been observed frequently in the field but has not been explained satisfactorily is the production of excessively high concentrations of ice crystals in certain clouds. Several mechanisms which would produce such an effect have been proposed. One such mechanism might be the mechanical fracturing of the fragile dendritic crystal types resulting from collisions with one another or with other crystal types. Basic to our understanding of such a process is an accurate knowledge of ice crystal terminal velocities. Detailed knowledge of the terminal velocities of ice crystals is important for additional reasons. It is a controlling factor in the growth of ice crystals by diffusion and accretion. In addition it is a controlling factor in the formation of ice crystal aggregates or snowflakes.

Despite the importance of the terminal velocities of ice crystals in so many cloud physics problems, our knowledge of them is very sparse and incomplete. The terminal velocities of several ice crystal types have been studied by Nakaya (1954). His work is generally regarded as the standard for ice crystal terminal velocities. Several other studies, Schaefer (1947), Magono (1953), and Litvinov (1956), have been reported on individual crystals, but these have not substantially altered Nakaya's results. Unfortunately however, Nakaya did not have a large data sample. In addition, more refined techniques than Nakaya used are now available for measuring the terminal velocity of ice crystals. For those crystal types not studied by Nakaya, the terminal velocities are not well known.

OBJECTIVES

The objective of this study has been to develop theoretical values for the terminal velocities of individual ice crystals and compare them with experimentally obtained values. To accomplish this, the following specific objectives have been to:

1. measure the terminal velocities of some of the crystal types reported by Nakaya using an improved technique which:
    a. reduces the human error factor,
    b. allows recognition of crystal accelerations,
    c. allows photographic determination of crystal type and size,
    d. allows determination of the falling attitude of crystals.
2. measure the terminal velocities of some of the crystal types not previously reported using the same technique.

BACKGROUND

The most extensive study on the terminal velocities of individual ice crystals was made by Nakaya (1954). He employed two techniques for determining the velocity. In one, crystals were dropped from the top of a closed tube and the time they took to fall through a distance of 2 meters was measured with a stopwatch. Graupel, which requires a considerable distance to reach terminal velocity, was measured by photographing falling pellets through a fan rotating at a known rate. The resulting streaks were chopped at known time intervals and the velocity then could be determined.

The results of Nakaya's work are shown in Fig. 1. Of particular interest are the curves for spatial and plane dendrites. They both show <u>no</u> size dependence. Nakaya's data is meager as he himself states and therefore is subject to further verification.

Schaefer (1947) photographed falling crystals that were illuminated by high pressure mercury lamps. The lamps were operated by an alternating current which produced a stroboscopic effect. With this he was able to determine the terminal velocities of a few individual crystals which he reported. For the most part his values were greater than those of Nakaya. Schaefer grouped crystals of various type together, which seriously reduces the value of his findings.

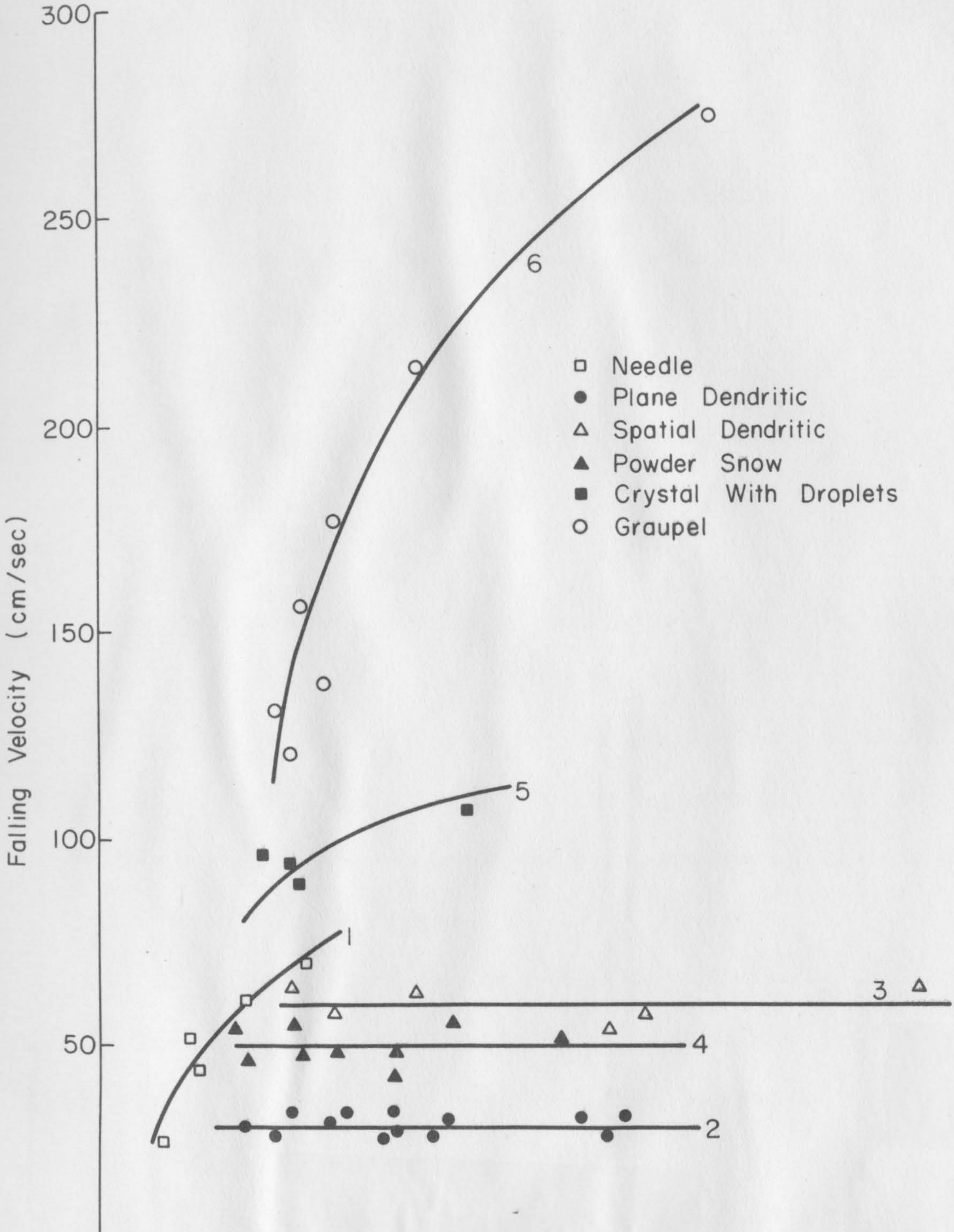

Figure 1. Rate of fall and dimension of various crystal types (Nakaya, 1954)

Magono (1953) worked primarily with snowflakes which are aggregates of individual ice crystals but did study a few individual crystals. His technique consisted of photographing the falling crystals which were illuminated once per .01 second with light produced by an electric discharge. Magono's results are similar to those of Nakaya.

In a later paper, Magono (1954) treated ice crystal terminal velocities from a theoretical standpoint. By making certain assumptions he was able to arrive at values which agreed quite well with Nakaya's findings.

Using an interesting technique, Langleben (1954) studied the terminal velocities of snowflakes. His method was to use a 16 mm cine-camera with a speed of 32 frames per second. The snowflakes were photographed in free fall against a dark background. Langleben found that the velocity of snowflakes was approximately equal to the 1/10 power of the snowflake mass.

Snowflakes were also studied by Litvinov (1956) using a 12 meter tube and a stopwatch to time the snowflake falling through the length of the tube. His results were similar to Langleben's, but they did not show as much dependence on size.

In a study of the fall velocities of plate-like and columnar ice crystals, Jayaweera and Cottis (1969) employed disk and column shaped objects, made of various materials, and allowed these to fall through fluids of different viscosities. From this work they were able to deduce certain characteristics which would allow them to predict the terminal velocities of plate and columnar ice crystals falling through air. They did not actually work with ice crystals but did check their predictions against nylon fibers falling through air and obtained good agreement.

Other investigations, similar to the one by Jayaweera and Cottis have been made. Podzimek (1968) studied the behavior of plastic and metal models falling through various fluids. His models simulated stellar, hexagonal plate, and plate with corner outgrowths types of ice crystals. Others, e.g. Stringham (1965), have studied the falling behavior of a wide range of shapes. These investigations were made for purposes other than the study of ice crystal behavior. However, they have proven very useful for predicting ice crystal terminal velocities.

THEORY

An object moving through a fluid experiences a resistance due to the behavior of the fluid. Shear stresses resulting from viscosity and velocity gradients along the surface of the object create forces tangential to the surface. Also affecting the object are forces normal to the surface which arise from pressure variations along the surface. The component of the vector sum of these forces directed opposite to the object's motion is usually known as the drag force, F_D. The drag force can be expressed as:

$$F_D = \tfrac{1}{2} C_D \rho A U^2 \tag{1}$$

where C_D is the drag coefficient, ρ is density of air, A is the cross-sectional area of the object normal to the direction of motion and U is the velocity of the object. The gravitational force G acting on the object is:

$$G = g(\rho_c - \rho)V \tag{2}$$

where g is gravitational acceleration, and ρ_c is the density of the object of volume V. When the object is falling at terminal velocity these two forces are equal. Thus:

$$\tfrac{1}{2} C_D \rho A U^2 = g(\rho_c - \rho)V \tag{3}$$

Solving (3) for U gives:

$$U = \left[\frac{2g(\rho_c - \rho)V}{C_D \rho A}\right]^{\frac{1}{2}} \tag{4}$$

This general expression for the terminal fall velocity is not readily suitable for computation because of the difficulty in assigning values to the drag coefficient for objects of various shape. This difficulty arises from the fact that the drag coefficient is a function of the object's velocity through its relationship with the Reynolds number, Re:

$$Re = d\,U/\nu \qquad (5)$$

where d is some characteristic length and ν is kinematic viscosity. The C_D-Re relationship is not expressable in terms of elementary functions but must be found experimentally.

Best (1950) developed an approach to solve this problem, which combines the Reynolds number and drag coefficient in the form:

$$X = C_D Re^2 \qquad (6)$$

where X is known as the Best number. Solving (3) for C_D and substituting this into (6) along with the expression for Re gives:

$$X = \frac{2d^2 gV}{\nu^2 A}\left[\frac{\rho_c - \rho}{\rho}\right] \qquad (7)$$

We can see that the velocity has conveniently dropped out and we are left only with terms which are easily evaluated. To use (7) for computing terminal fall velocities, the X-Re relationship for the shape in question is necessary. This is readily found if the C_D-Re relationship is known for the particular shape. The procedure is to calculate X for a given object, then find the corresponding value of Re and calculate U from the expression for Re.

In the remainder of this section, an attempt has been made to determine the relationship between terminal fall velocity and ice crystal size for various crystal types using Best's technique. To do this the work of several authors on the C_D-Re relationship of various shaped objects has been utilized. The results are shown graphically along with the experimental values obtained in this study.

Plane Dendrites

It was found by Magono (1953) and confirmed in this study that plane crystals fall with their basal face horizontal. This was predictable from the work of various authors on thin disks falling through viscous fluids, e.g. Stringham (1965). He found that when Re< 100, disks fall with their maximum cross-sectional area normal to the direction of motion in a steady fashion, but when Re exceeds 100, the disks begin to oscillate slightly and increase their erratic behavior as Re increases. The value of Re for most plane crystals is < 100, with only those crystals greater than about 3-4 mm in diameter exceeding this value. For those, the oscillations are small and about the vertical and thus do not effect their horizontal attitude. Fig. 2 is a photograph of a falling dendrite which was illuminated every 1/100 of a second by a strobe light. It clearly demonstrates the horizontal attitude of the basal plane.

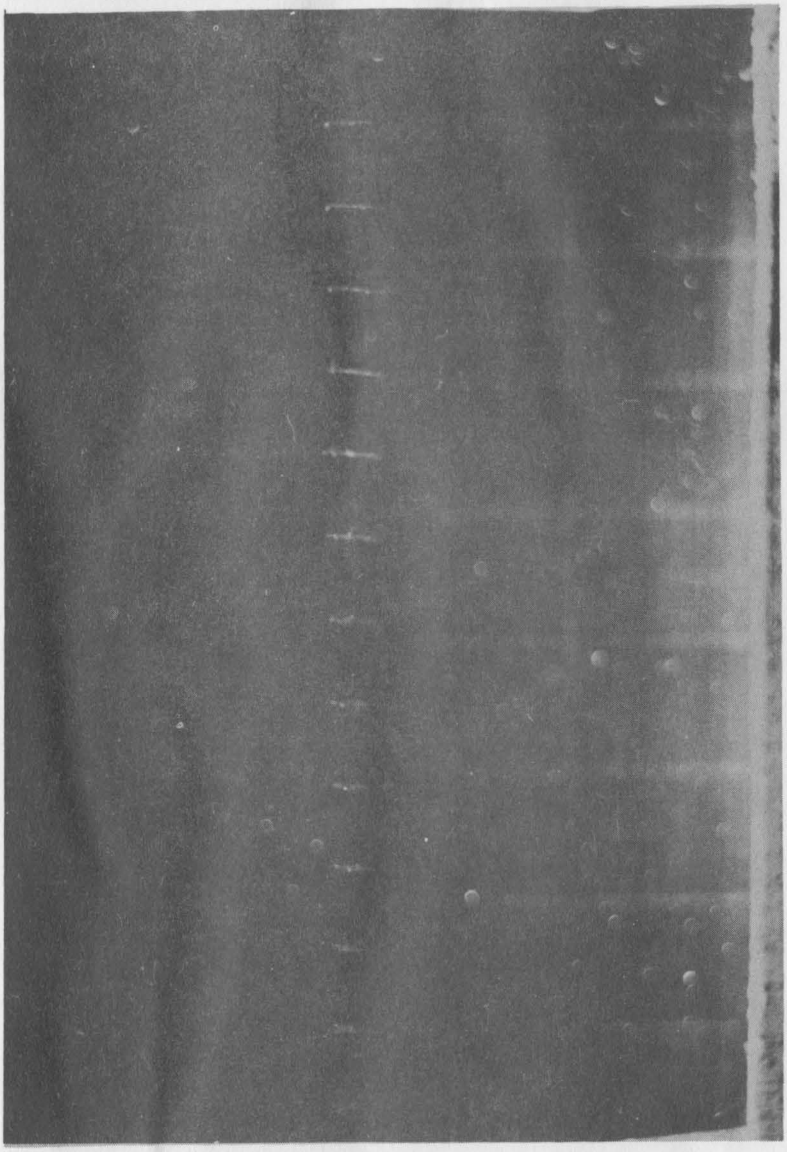

Figure 2. Falling plane dendrite showing horizontal attitude.

The cross-sectional area normal to the direction of motion then is simply the area of the basal plane. Since the volume of the crystal is the basal area times the thickness, the ratio V/A reduces to just t, the crystal thickness. Thus for plane dendrites, (7) becomes

$$X = \frac{2d^2 tg}{\nu^2} \left[\frac{\rho_c - \rho}{\rho} \right] \tag{8}$$

The relationship between crystal diameter and thickness has been investigated by several authors. Auer and Veal (1970) have made the most extensive study and report that the thickness slowly increases as the diameter increases. Ono (1969) found that plane crystals show an increase in thickness as the diameter increases until they reach 50-60μ thick. This occurs at a diameter of about 1600μ. The apparent discrepancy between the two investigations can probably be explained by the small sample size obtained by Ono. Plotting Ono's curve on the diagram of Auer and Veal shows that it lies within the scatter of their points. The two curves are shown in Fig. 3. Reynolds (1952) in a study of plane crystals nucleated in a cold chamber, obtained results which agreed quite well with Ono for very small crystal diameters. His results are shown in Fig. 4. However, Nakaya (1954) reported an average thickness for dendrites of 11μ. The reason for this wide departure from the results of others is not obvious.

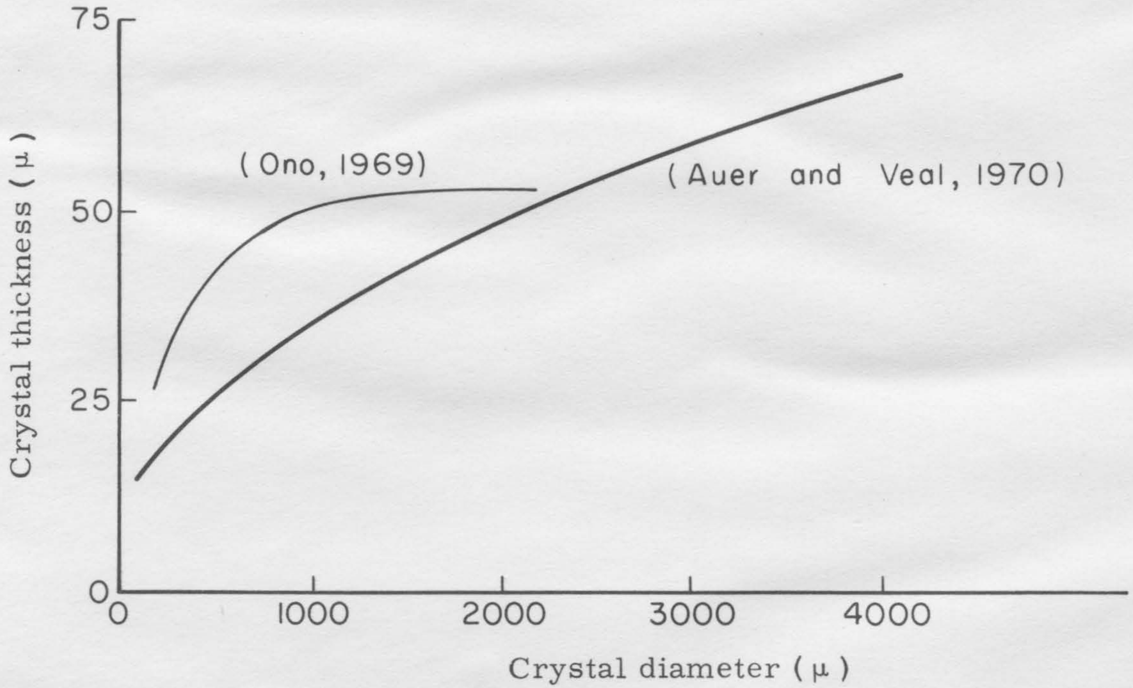

Figure 3. Relationship between the thickness and diameter of plane ice crystals

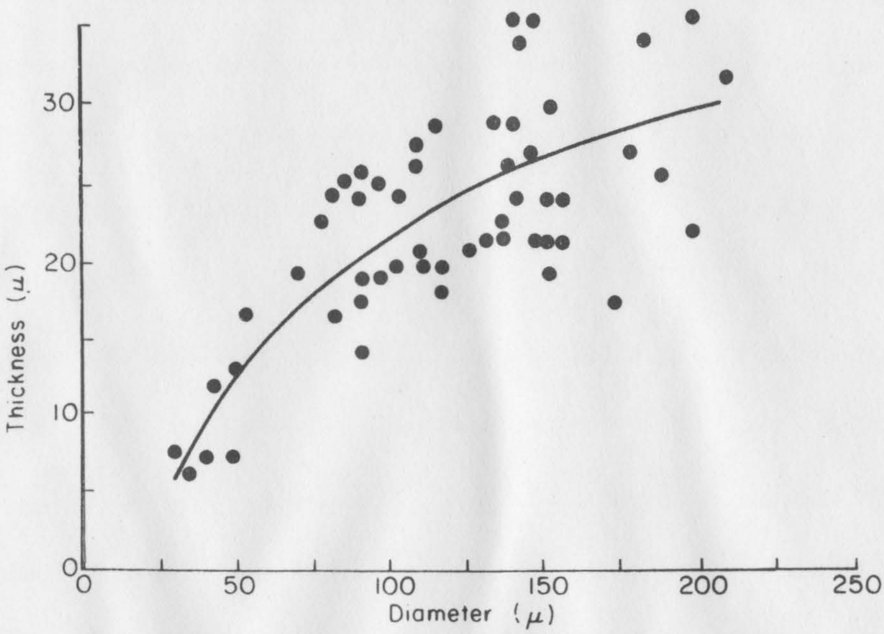

Figure 4a. Measured relation between thickness and diameter of plane dendritic crystal forms (Reynolds, 1952)

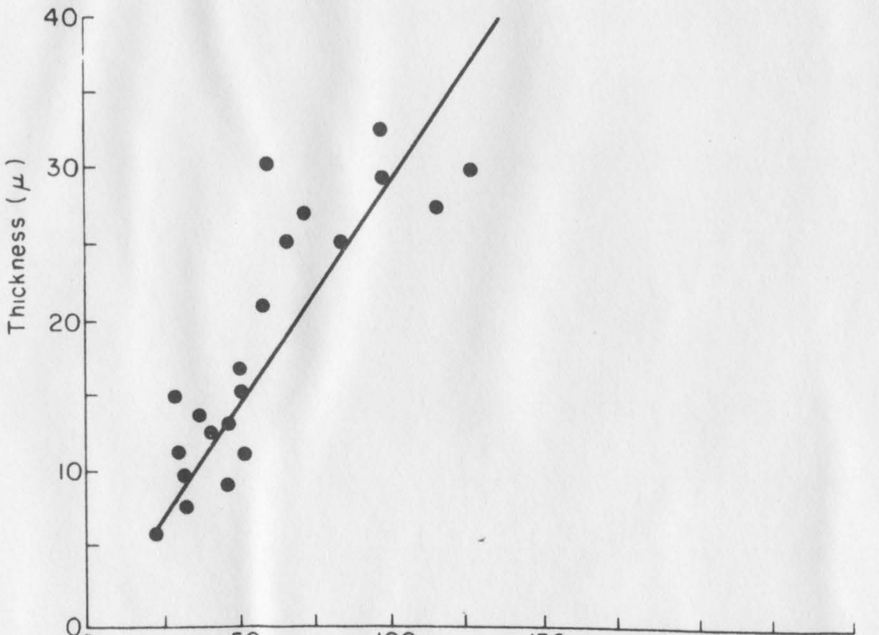

Figure 4b. Measured relation between thickness and diameter of hexagonal plate crystal forms (Reynolds, 1952)

Podzimek (1968) has determined the drag coefficient-Reynolds number relationship for models which simulated hexagonal plates, both with and without corner outgrowths, and stellars. He gives the relationship for plates as: $C_D = 16.5\ Re^{-.466}$ and for stellars and plates with outgrowths: $C_D = 20.2\ Re^{-.466}$. These relationships are plotted in Fig. 5 using log-log scales. From these curves, the X-Re relationships were determined and these are also shown in Fig. 5. Using values of t from the curve of Auer and Veal to calculate X and then finding the corresponding value of Re from the X-Re curve for stellars in Fig. 5 the relationship between terminal fall velocity and crystal diameter was found. This is shown in Fig. 12. It should be emphasized that this curve is valid only for crystals exhibiting a diameter-thickness relationship which is in agreement with Auer and Veal. Crystals which exhibit a different diameter-thickness relationship, such as reported by Nakaya, would lie along another curve.

Hexagonal Plates

The expression for the Best number given by (8) applies to plates as well as plane dendrites. Following the same procedure used for plane dendrites, the terminal velocity-crystal diameter relationship was computed. This relationship is shown in Fig. 12 also. The two curves are similar in shape, with the plate curve being somewhat higher due to plates having a lower drag coefficient

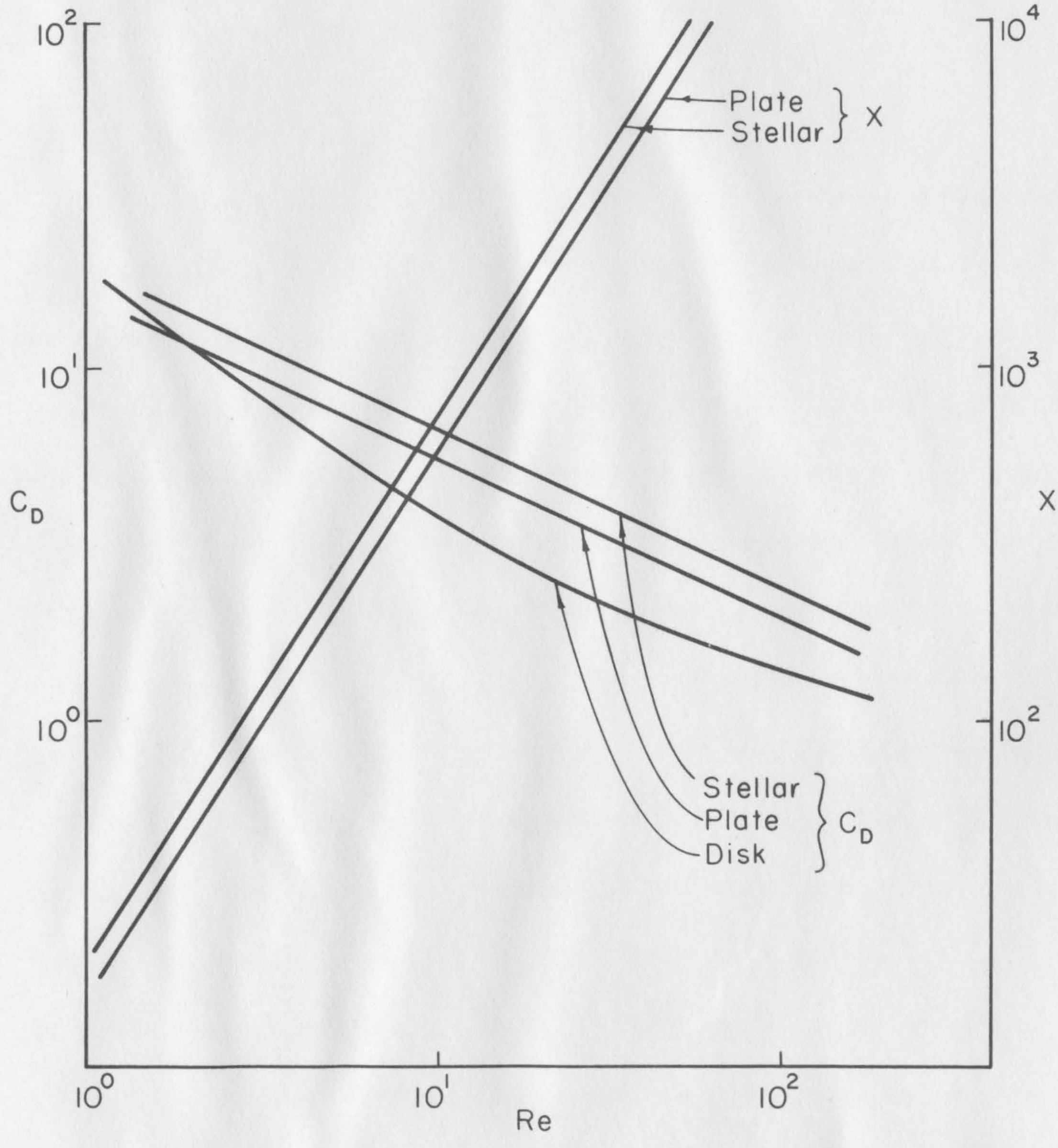

Figure 5. C_D-Re and X-Re relationships for stellars and plates as found by Podzimek (1968). Also shown is the C_D-Re relationship for thin circular disks

than plane dendrites. Again it should be emphasized that this curve holds only for those crystals which exhibit the diameter-thickness relationship found by Auer and Veal.

Spatial Dendrites

When spatial dendrites are considered, the problem becomes more complex. Because of the random orientation and number of arms occurring, it is not possible to define cross-sectional area and volume as simply as for plane crystals. To overcome this difficulty, the problem can be approached in the following manner: the spatial dendrite can be considered in terms of a sphere which would just enclose it. A certain fraction of the sphere's volume would be ice and the remainder air. Likewise, if we project the crystal arms on a cross-section through the sphere, a fraction of the cross-sectional area would be ice and the remainder air. However, the area of ice would vary depending on the orientation of the cross section. Although the area of ice varies, a mean value will exist for each crystal. Letting the fraction of the volume which is ice be x, and the mean fraction of the area which is ice be $\overline{y}$, an expression for the volume of a spatial dendrite can now be written as:

$$V = x\, 4/3\, \pi r^3 \tag{9}$$

where r is the radius of the sphere which just encloses the crystal. Likewise the expression for the mean cross-sectional area is:

$$A = \overline{y}\, \pi r^2 \tag{10}$$

These results can now be incorporated into (7) giving:

$$X = \frac{32\, r^3 g}{3\nu^2} \left[\frac{\rho_c - \rho}{\rho}\right]\left[\frac{x}{\bar{y}}\right] \tag{11}$$

Before (11) can be used, the factor $(x/\bar{y})$ must be evaluated. If we consider a simple six branch crystal, four branches lying in one plane and the other two perpendicular to it, an approximate value for $(x/\bar{y})$ can be obtained. First, looking at a broad branch crystal, much like those found in this investigation, and using the following dimensions: branch width: 500μ; branch length: 1000μ; branch thickness: 50μ, x is found to have a value of .003.

As mentioned earlier, y varies depending on what cross section is taken. y will be near a minimum when the cross section is taken perpendicular to a branch such that the remaining branches are seen on edge. This is shown in Fig. 6a. Actually, y would be slightly less if the crystal was rotated 45° about the vertical. The maximum value will occur when the cross-section is again taken perpendicular to a branch but in such a manner that the remaining branches have their broad faces parallel to the cross-section as shown in Fig. 6b. The first condition gives a value of .06 for y while the second gives .56. Using these values to compute $x/\bar{y}$ gives .05 in the first case and .0053 in the second. Thus $x/\bar{y}$ will have a value somewhere in between .05 and .0053. Further calculations show that as the branches become more slender, $x/\bar{y}$ increases rapidly.

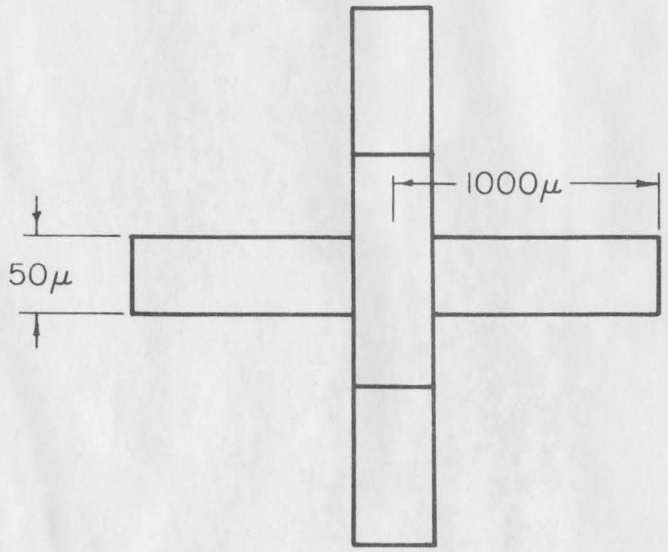

Figure 6a. Cross section of spatial dendrite showing minimum y

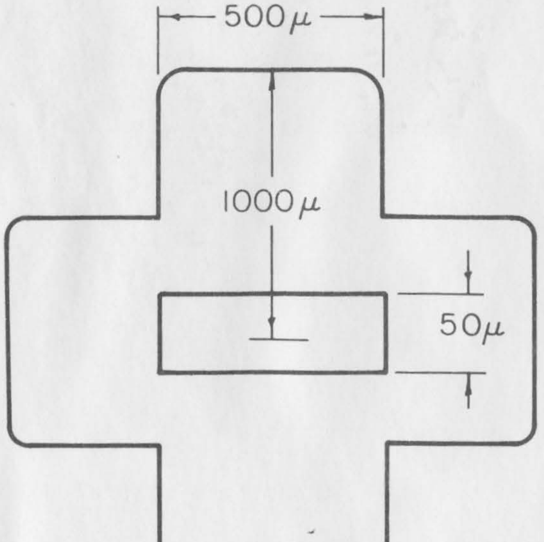

Figure 6b. Cross section of spatial dendrite showing maximum y

The problem now arises of what X-Re relationship to use. The author was unable to find any information on this relationship for objects similar in shape to spatial dendrites. As a first approximation, the relationship for stellars shown in Fig. 5 can be used.

This approximation is probably quite realistic. If the spatial dendrite consists of six arms, it will have approximately the same surface area as a plane dendrite of similar branching. Thus the area over which frictional drag occurs would be essentially the same for both crystals. However, the cross-sectional area presented to the flow by the spatial dendrite would be less than that of the plane dendrite since all six arms of the spatial dendrite do not lie in the same plane. Thus the area over which pressure drag occurs is less for the spatial dendrite. At low Reynolds numbers the frictional drag is much greater than the pressure drag. As the Reynolds number increases, the pressure drag becomes more significant in relation to the frictional drag and at a certain value of the Reynolds number, becomes the dominant factor. However, the value of the Reynolds number at which this occurs for objects shaped like spatial dendrites is not known. The fact that plane dendrites have higher drag coefficients than hexagonal plates indicates that the frictional drag is still the dominant factor for the range of Reynolds numbers covering these crystals. It is believed that this conclusion can be safely extended to spatial dendrites. Thus we can expect the drag force on both plane and spatial dendrites to be quite similar.

Using this approximation and allowing $x/\overline{y}$ to take on various values, we can compute the relationship between the terminal velocity and the measure of crystal size r. A different relationship exists for each value of $x/\overline{y}$ and several of these are plotted in Fig. 14.

Columns and Needles

Stringham (1965) found that columns fall with their longest or 'c' axis horizontal when the Reynolds number is between 10 and 400. Ono (1969) found this also for the case of columnar ice crystals. Thus the cross-sectional area normal to the direction of motion is the length times the crystal width. The width is the diameter of a circumscribed circular cylinder which just encloses the crystal. The cross-sectional area can then be expressed as:

$$A = 2RL \tag{12}$$

where R is the radius of the circumscribed cylinder and L is the crystal length. The volume is:

$$V = \frac{3\,[3]^{\frac{1}{2}}}{2} R^2 L \tag{13}$$

Substituting these into (7) gives:

$$X = \frac{6\,[3]^{\frac{1}{2}} R^3 g}{\nu^2} \left[\frac{\rho_c - \rho}{\rho} \right] \tag{14}$$

Equation (14) shows the interesting result that X is dependent on the crystal radius and not directly on length.

Ono (1969) has found the relationship between length and diameter of a large number of columns. His results are shown in Fig. 7. We can see that columns reach a maximum diameter of about 90μ although the length may continue to increase. Thus two crystals of the same diameter may have quite different lengths and yet will have the same Best number. However, Jayaweera and Cottis (1969) have obtained the X-Re relationship for circular cylinders and report that at low values of X, the relationship is markedly dependent on the length/diameter ratio but becomes less dependent as X increases. Their results are shown in Fig. 8. Using this information they plotted curves of terminal fall velocity versus L/d ratio for cylinders of various diameter. These are shown in Fig. 9.

The more recent study by Auer and Veal (1970) does not reveal the cutoff of crystal growth in the 'a' direction at 90μ. Rather their results showed a gradual increase in diameter as length increased. Both Auer and Veal and Ono obtained a large number of observations. Thus this question remains to be resolved.

Needles are treated in the same manner as columns, being classified as columns with much greater length than diameter by Jayaweera and Cottis (1969). However in the study by Auer and Veal (1970) it was found that the L/d ratio of needles varied from about five for the shortest length crystals to approximately 40 for the maximum length crystals. At the same time the L/d ratio of

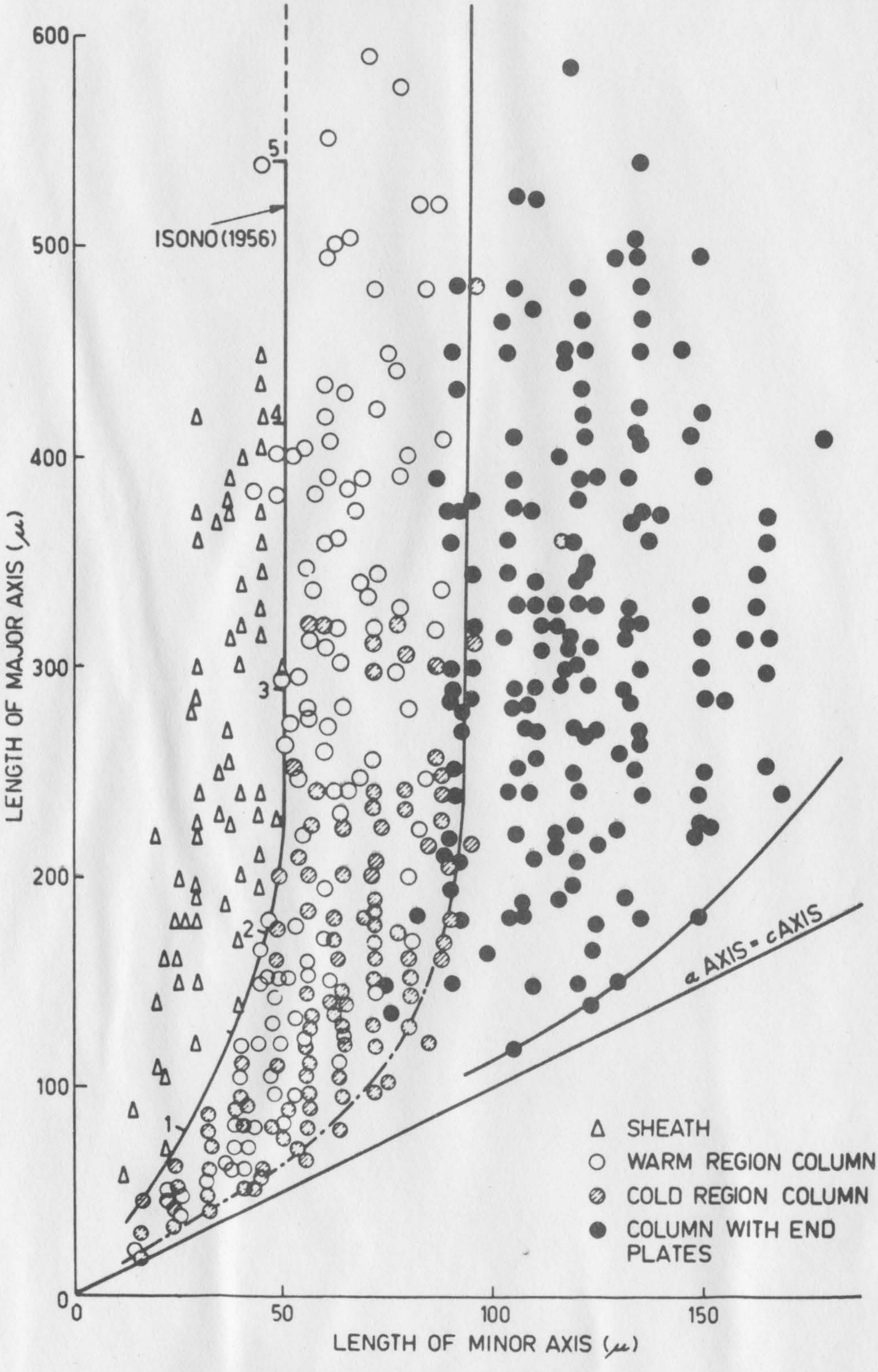

Figure 7. Relationship between length of major and minor axis of columns (Ono, 1969)

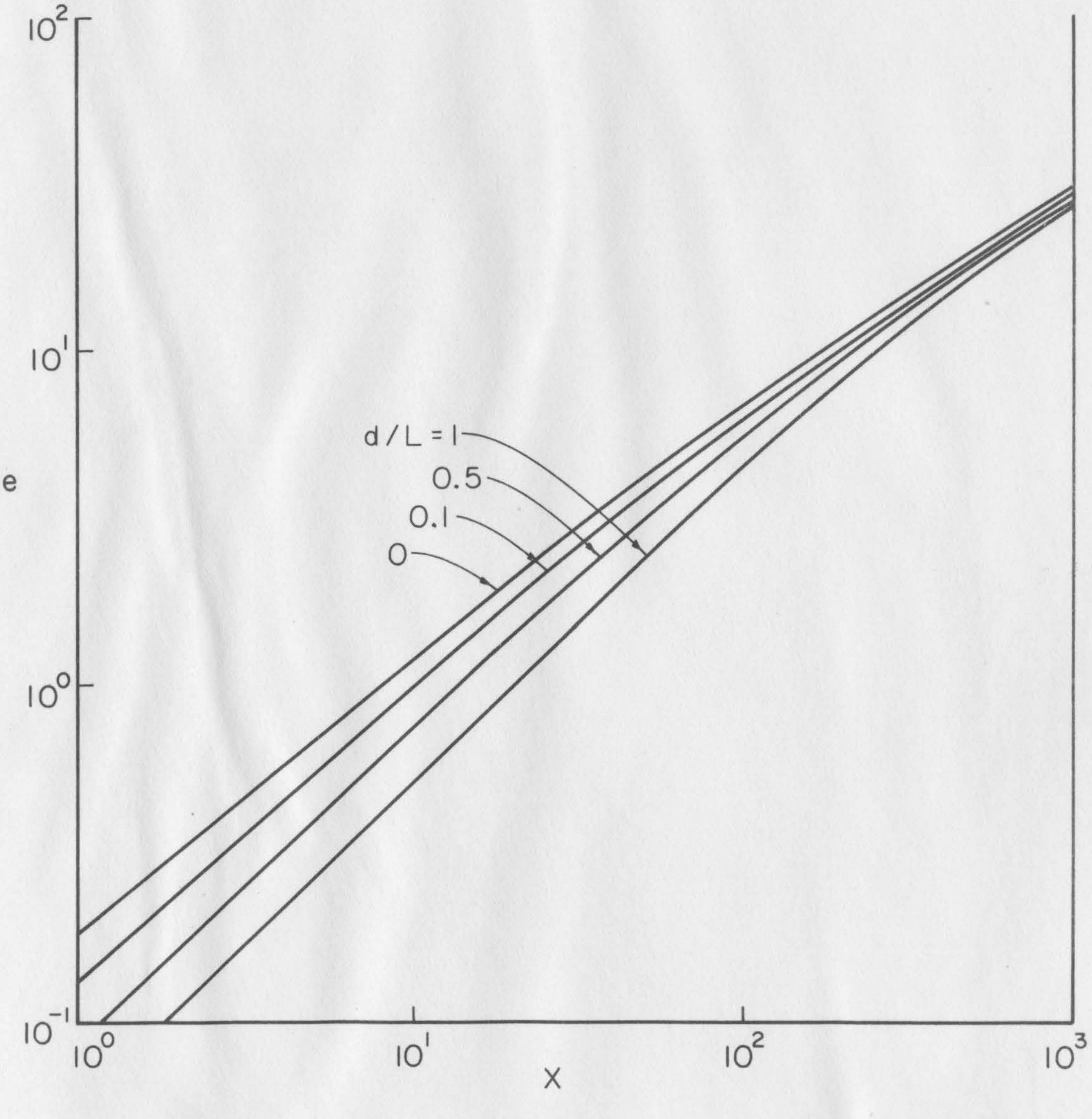

Figure 8. Relationship between X and Re for cylinders of various d/L ratio as found by Jayaweera and Cottis (1969)

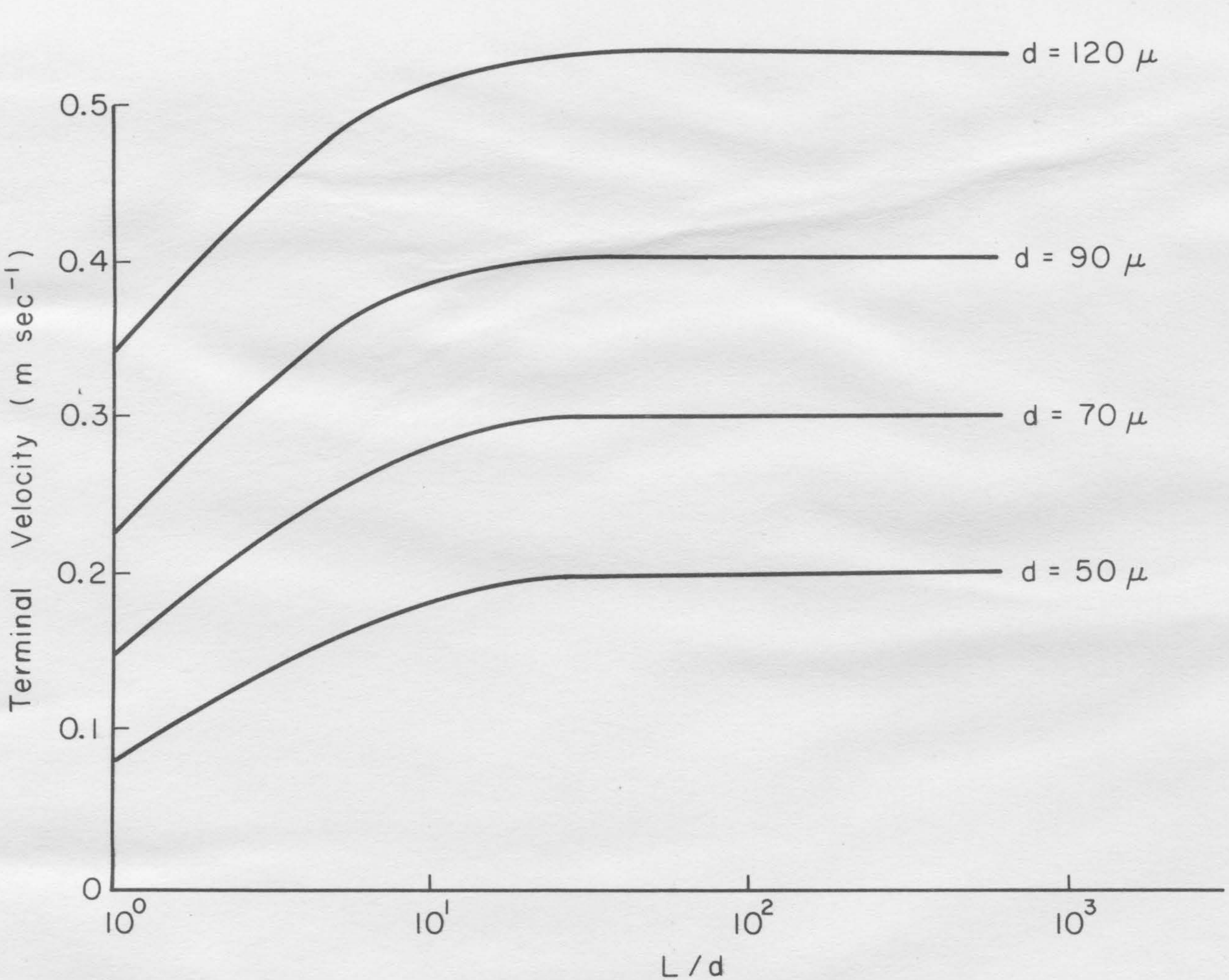

Figure 9. Computed terminal velocities of cylinders of various diameters as a function of L/d (Jayaweera and Cottis, 1969)

columns varied from 2 to 15. Thus such a simple definition as stated by Jayaweera and Cottis is not adequate.

Capped Columns

Ono (1969) has reported that capped columns fall with the column length oriented vertically. Thus the cross-sectional area, normal to the direction of motion, is the area of the basal plane of the plate capping the column. Letting R be the radius of a cylinder which circumscribes the column and R' be the radius of a thin disk which circumscribes the end plates, the expression for the crystal volume is:

$$V = \frac{3\ [3]^{\frac{1}{2}}}{2} R^2 L + 3\ [3]^{\frac{1}{2}} R'^2 h \qquad (15)$$

where L is the column length and h is the plate thickness. The cross-sectional area of the bottom plate is:

$$A = \frac{3\ [3]^{\frac{1}{2}}}{2} R'^2 \qquad (16)$$

Substituting into (7) gives:

$$X = \frac{8 R'^2 g}{\nu^2} \left[\frac{R^2 L}{R'^2} + 2h\right]\left[\frac{\rho_c - \rho}{\rho}\right] \qquad (17)$$

Information on the X-Re relationship is not available for objects of this shape. However, by making certain assumptions it is possible to predict how the X-Re relationship will compare with those of other shapes. Due to the falling attitude of a capped column, the air will flow around the bottom plate. If the crystal falls with sufficient speed, wake formation will occur, and if great enough no further contact between air and crystal will occur after the air passes from the edge of the bottom plate. If these conditions are met, the drag on the crystal will consist entirely of pressure drag on the basal face. The crystal will then be expected to behave like a thick plate with mass equal to that of the capped column. Of course, this concept required many assumptions to be made. In addition, little is known on the relationship between R, R', L, and h. Because of this uncertainty, it seems rather pointless to attempt to compute the relationship between terminal velocity and various crystal dimensions.

Graupel

The approach used for computing the terminal velocity of spatial dendrites can be readily applied to graupel because of its irregular shape. Considering a sphere which just encloses the particle, a fraction x of the sphere's volume would be ice and the remainder air. In similar fashion, a cross section through the sphere would have a fraction y of its area ice and the remainder air. Again, as with spatial dendrites, the value of y would vary as the orientation of the cross-section changed. However, a mean value, $\overline{y}$, would exist and this would be a constant for a given particle. Expressions for the volume and area are identical with equations (9) and (10) and when substituted into equation (7) give the result:

$$X = \frac{32\, r^3 g}{3\, \nu^2} \left[\frac{\rho_c - \rho}{\rho} \right] \left[\frac{x}{\overline{y}} \right] \qquad (18)$$

which is identical with equation (11). Of course the factor $x/\overline{y}$ will be different for graupel, as well as the density ρ_c.

The greatest problem in treating graupel theoretically arises from the density, because of its wide variation. Nakaya reported an average value of .125 g/cm^3 while Braham (1964) found values near .9 g/cm^3 in summer cumulus. This variation in density would cause a large difference in fall velocities between the particles studied in the respective investigations.

EXPERIMENT

The basic method used for determining the terminal velocities of ice crystals consisted of photographing a falling crystal using a strobe light for illumination. To do this, a means of controlling the position of crystals falling in front of the camera was necessary. Also required was a way in which the crystal could be illuminated by the strobe light while at the same time the camera could be shielded. Thirdly, a means of determining the distance that the crystal fell between strobe flashes was necessary.

Instrumentation

These requirements were met by constructing a 9 cm x 27 cm x 15 cm "black box". At one end a 35 mm camera was mounted. Towards the other end, a vertical slit, open at the top and bottom, was made with glass plates. The box design is shown in Fig. 10. A 1 cm^2 grid was attached to the plate at the back of the slit to allow the distance determination discussed above. One side of the slit contained a glass window for illumination of falling crystals by the strobe light. The camera was focused in the middle of the 1.5 cm wide slit and exposure times ranged from $\frac{1}{2}$ to 3 seconds depending on film speed and crystal source. Image clarity was quite good and in most cases natural crystals could be readily identified from the film. The result of this arrangement was a series of images of the same crystal falling in front of the grid. An example of this is

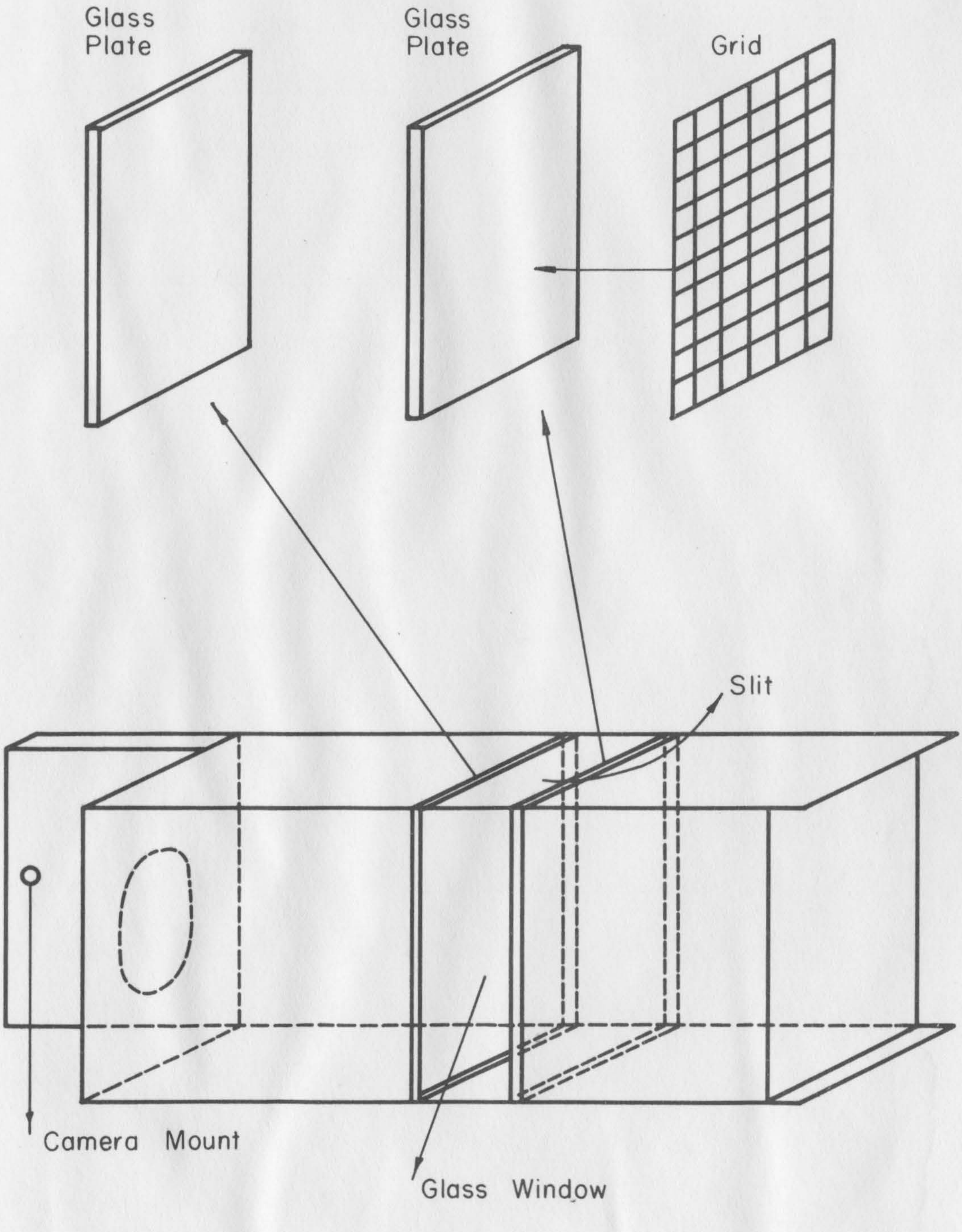

Figure 10. Design of "black box"

shown in Fig. 2. The distance between images was determined from the grid while the time between images was known from the strobe light frequency. Thus only a simple calculation was necessary to find the fall velocity of the crystal. The box and camera were mounted on a stand and a plastic tube was placed above the slit to eliminate horizontal drafts. It was possible to close the bottom of the slit as well as the top of the tube when windy conditions required it. The physical arrangement of the apparatus is shown in Fig. 11.

Procedure

Two crystal sources were used and the procedure that was followed varied somewhat depending on source. Natural plane dendrites were collected and stored in sealed plastic containers in a cold chamber for later use. To study them, the apparatus was set up in the cold chamber at a temperature of about -20°C. Wind conditions were calm so the bottom of the slit was left open. To eliminate thermal effects, the apparatus was allowed to cool overnight before proceeding. The dendritic crystals were dropped one at a time and caught at the bottom of the slit on a glass slide. A photomicrograph was then made for later comparison of size with that determined from the photograph of the falling crystal.

The other crystal types studied empirically were photographed as they fell in natural snowfall. This included spatial dendrites, capped columns, needles, needle bundles, and graupel. To

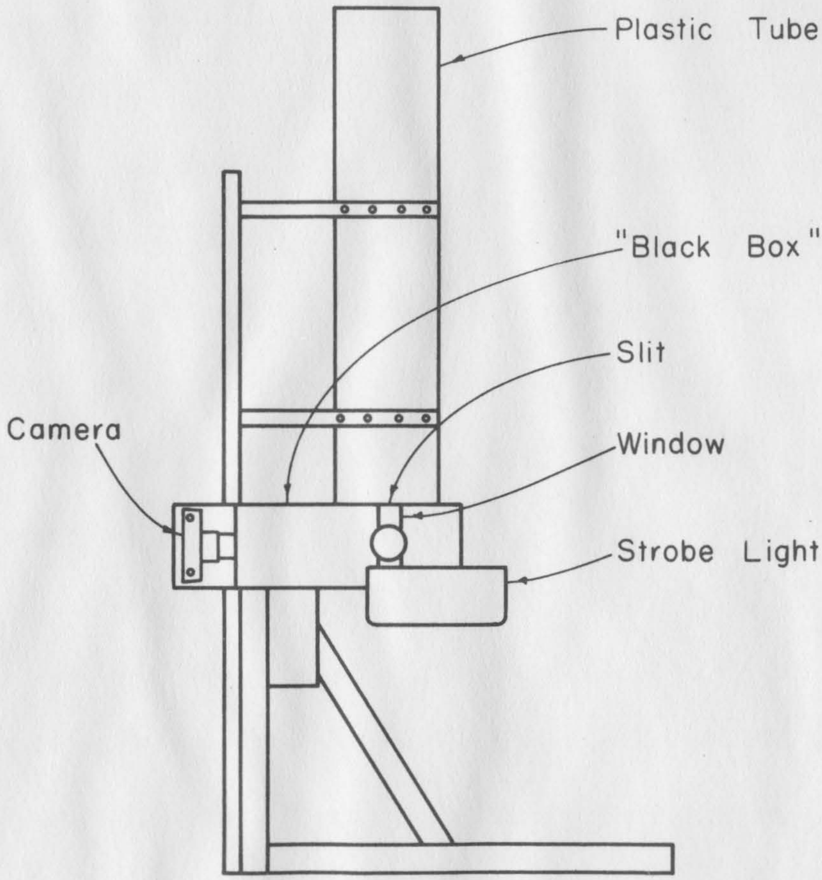

Figure 11. Physical arrangement of experimental apparatus

eliminate possible air motion within the chamber the slit bottom was kept closed. The tube top opening was also reduced in size. To enhance the possibility of photographing a crystal, a slow speed film and exposure time of 3 seconds were used under these conditions.

A constant strobe light frequency of 6000 c.p.m. was used throughout the study. This produced several images of the fastest particles while at the same time it maintained adequate separation of the images of the slower particles. It should be pointed out that one distinct advantage of the method employed in this study was that particle accelerations were recognizable from variations in separation of the crystal images.

To check the repeatability of the procedure, several dendritic crystals were dropped through the apparatus more than once. No difference in terminal velocity was detectable between each trial, thus increasing the author's confidence in the method.

RESULTS AND DISCUSSION

Plane Dendrites

Approximately 100 plane dendrites were photographed. All but 41 of these either showed riming or hit the slit edge. The experimentally determined values for these 41 are plotted in Fig. 12. While the observations show greater velocities than those of Nakaya as predicted by theory, agreement with the computed curve is rather poor. The fact that the experimental data is, in general, below the computed curve indicates that the actual dendrites had a higher drag coefficient than the stellar models used by Podzimek although it might be partly due to a difference in thickness since he does not provide this information on his models. The disagreement between the slope of the computed curve and the general slope of the author's data can perhaps be attributed to the C_D-Re relationship reported by Podzimek. This relationship gives a curve of constant slope when plotted on log-log paper. However, the C_D-Re relationship as found by various authors, for objects of other shape shows a significant change in slope as Re varies up to Re $\simeq 10^3$. The relationship for a thin circular disk which closely approximates a hexagonal plate in shape is shown in Fig. 5.

To see what effect this had, a curve, parallel to the C_D-Re curve for thin disks and tangent to Podzimek's curve, was drawn. From this a new X-Re curve was obtained and finally the resulting terminal fall velocity-diameter relationship was computed. This new relationship is the starred curve shown in Fig. 12. We see that

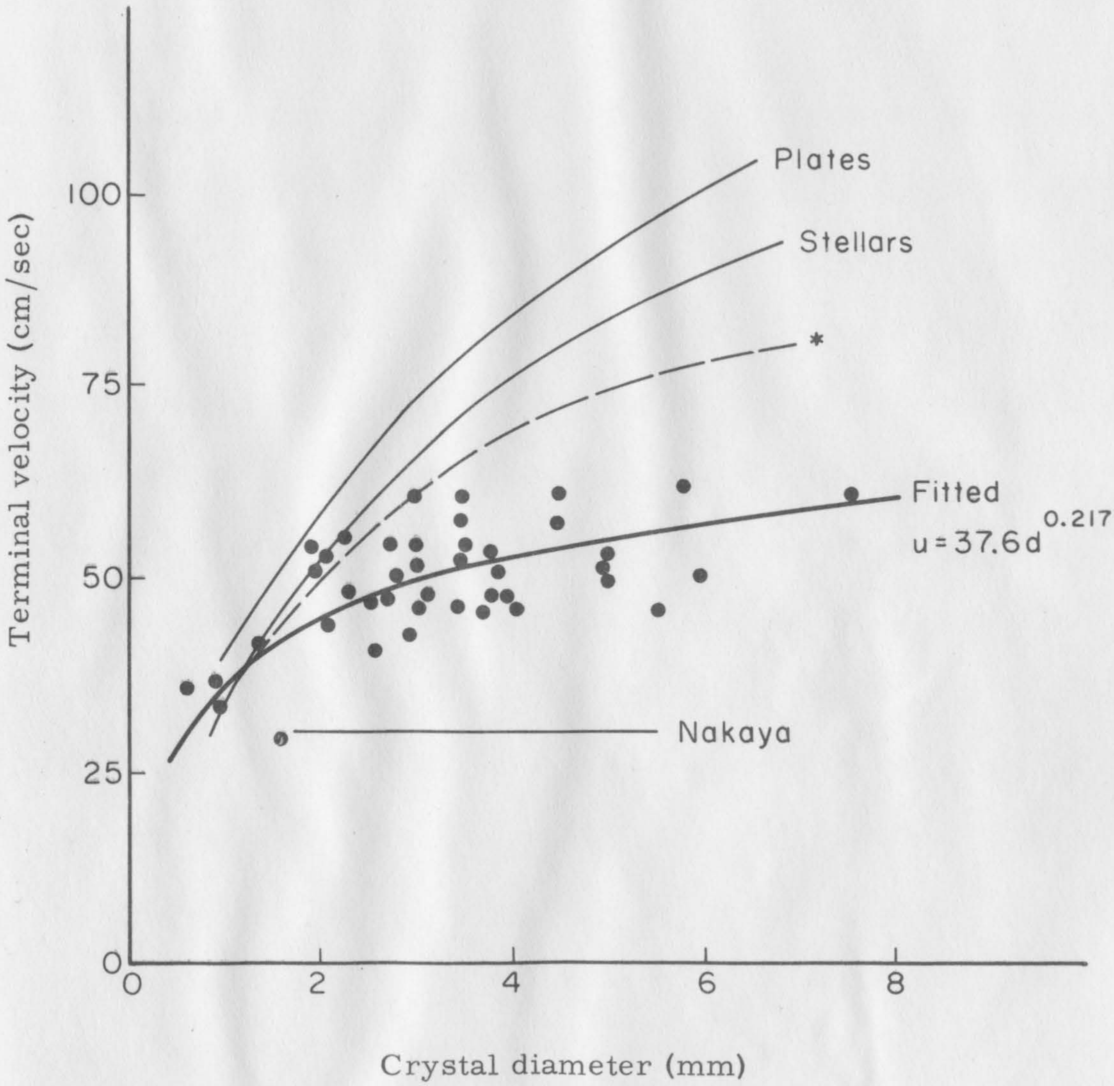

Figure 12. Relationship between terminal velocity and crystal diameter of unrimed plane dendrites and plates

* See text for explanation of this curve

there is better agreement between the slope of the new computed curve and the slope of the experimental data. Of course the position of the new curve is of less significance since the choice of position of the C_D-Re curve was arbitrary.

Also shown in Fig. 12 is a fitted curve using the least-squares method as well as Nakaya's curve. The large difference between Nakaya's results and those obtained in this study are in part due to the difference in elevation between the two experimental sites but this would only amount to about 2 cm/sec. Of more significance is the difference in crystal thickness found in the two studies. A few dendrites collected in this study were observed to determine their thickness and were found to agree quite well with Auer and Veal. However, as mentioned earlier, Nakaya reported that the average thickness of the dendrites which he studied was 11μ. The fact that Nakaya's curve shows a constant terminal fall velocity can probably be explained by 1) the fact that his data sample was small and 2) the size dependence is actually quite small for crystals larger than 1600μ in diameter, the range in which Nakaya made his measurements. It is also possible that the crystals had not reached terminal velocity when Nakaya began his timing, since they had fallen only 20 cm at this time. His technique did not allow recognition of crystal accelerations such as was possible with the technique used in this study.

A few of the dendrites showed a small amount of riming as noted from the photomicrographs. These were excluded from the unrimed dendrites. However, due to the importance of accretion processes, a plot of their terminal velocities versus crystal diameter was made as shown in Fig. 13. It is apparent that even though a large amount of scattering is present, in general the values are considerably higher than those found for unrimed dendrites.

Theoretically the riming can be treated as an increase in crystal thickness equivalent to the total volume of the rimed droplets. This is a result of the rime occurring primarily on the basal face. Due to the variation in the amount of riming, one would expect a variation in terminal velocities, as observed.

Spatial Dendrites

The data obtained for 40 spatial dendrites are shown in Fig. 14. We see that the crystals exhibit $x/\overline{y}$ ratios between .03 and .09 with a tendency towards lower values as the crystal size increases. It is not known how this ratio varies with crystal size nor under different growth conditions. It appears that it does not remain constant as the size increases, however this may be due to the shape of the C_D-Re curve plotted from Podzimek's expression as discussed in the previous section. If the C_D-Re curve showed the same change in slope as curves for other shapes, then the computed curves in Fig. 14 would exhibit a greater change in slope and would be closer

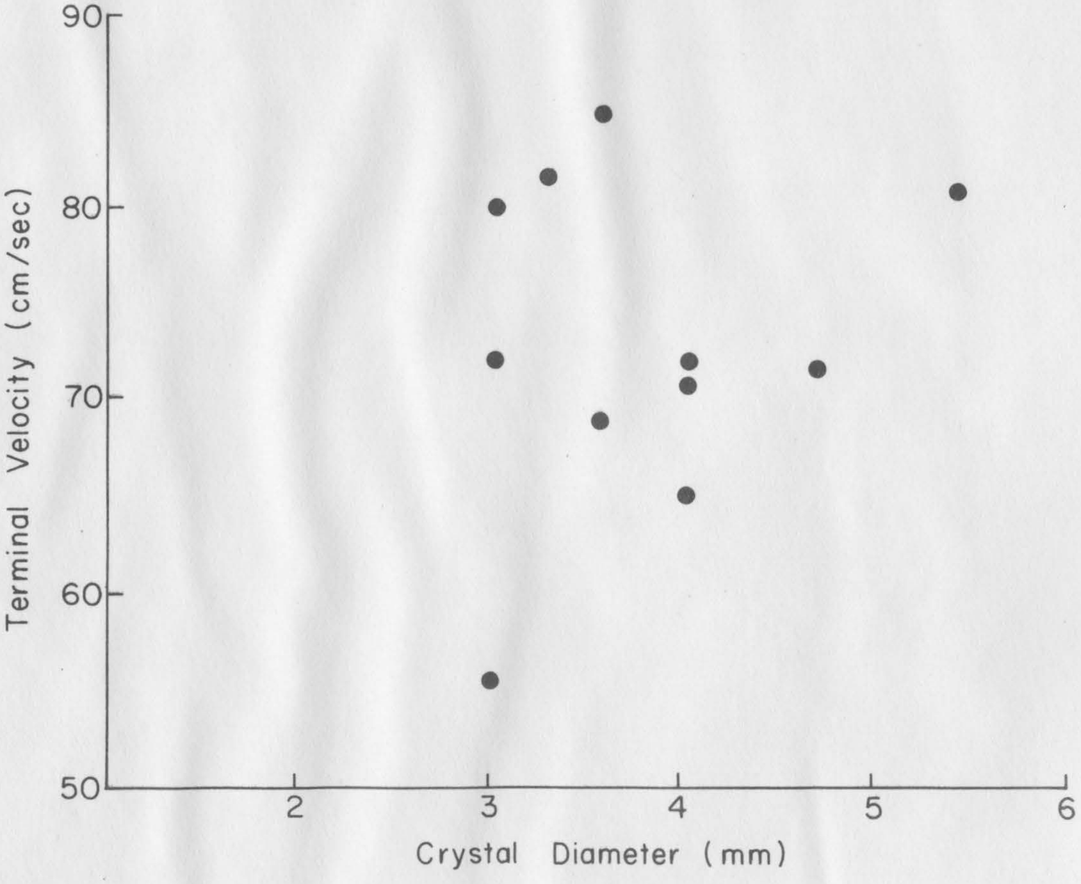

Figure 13. Relationship between terminal velocity and crystal diameter of rimed plane dendrites

to the experimental data. An example of this has been computed and is shown in Fig. 14. Also shown are the findings of Nakaya and a curve which was fitted to the data.

Needles

Unfortunately only three falling needles were photographed in this study. As expected they fell with their 'c' axis horizontal. Their terminal fall velocities are plotted in Fig. 15 along with Nakaya's findings. The values appear to agree quite well with Nakaya if his curve is extended to larger sizes. Three needle bundles were also photographed and these are included in Fig. 15.

Capped Columns

Several falling capped columns were photographed and their terminal fall velocity as a function of column length is shown in Fig. 16. In addition several crystals consisting of more than one column, separated by plates in a stacked fashion, were photographed. An example of these is shown in Fig. 18. Their terminal fall velocities are shown in Fig. 17.

As discussed in the theory section, if the crystal fell with sufficient speed to cause wake separation to occur, we would expect the crystal to behave as a thick plate of mass equal to that of the capped column. Such a crystal would, of course, have a greater terminal fall velocity than the plates in Fig. 12 and would also show dependence on the column length L through its effect on the crystal

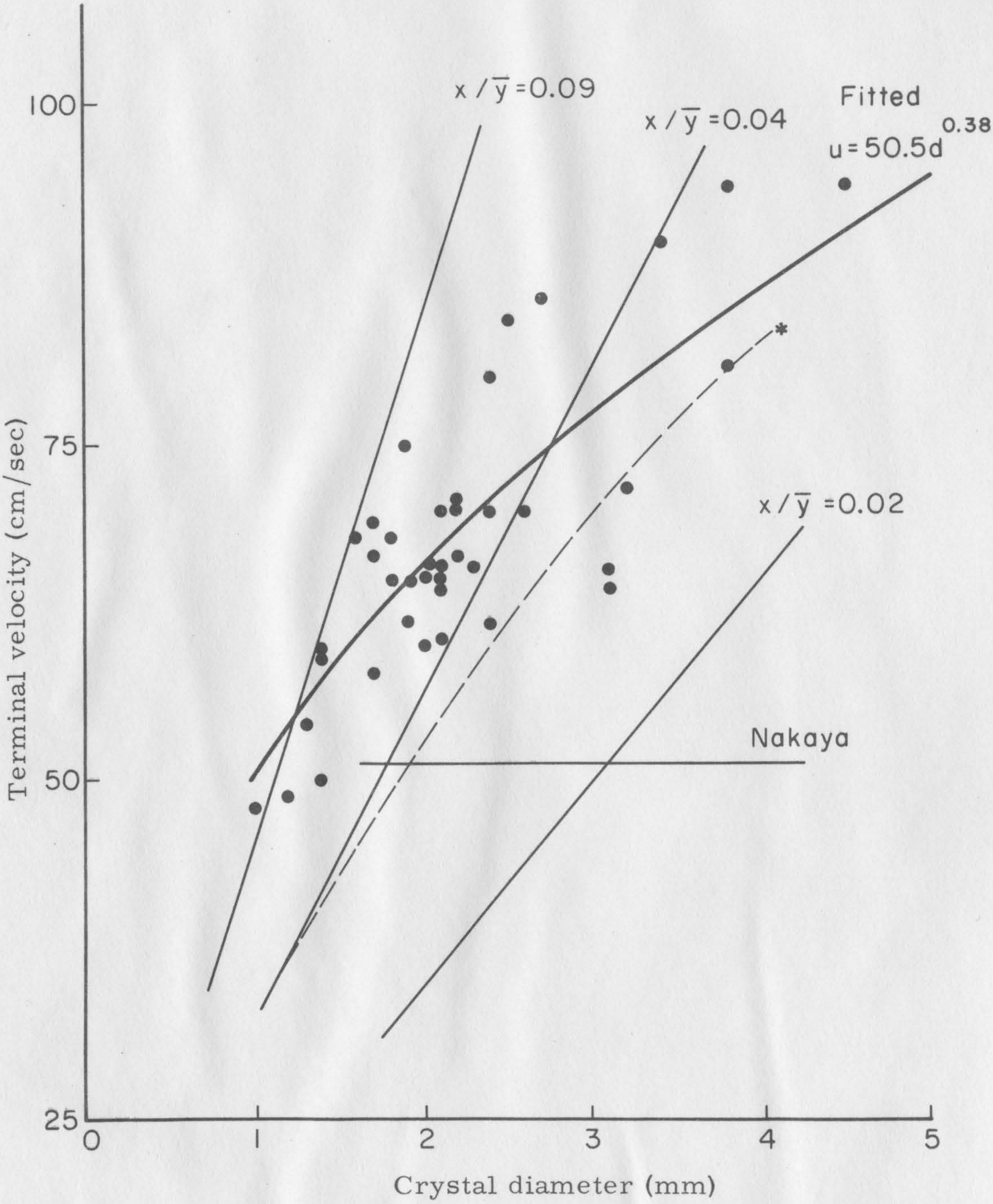

Figure 14. Relationship between terminal velocity and crystal diameter of spatial dendrites

* See text for explanation of this curve

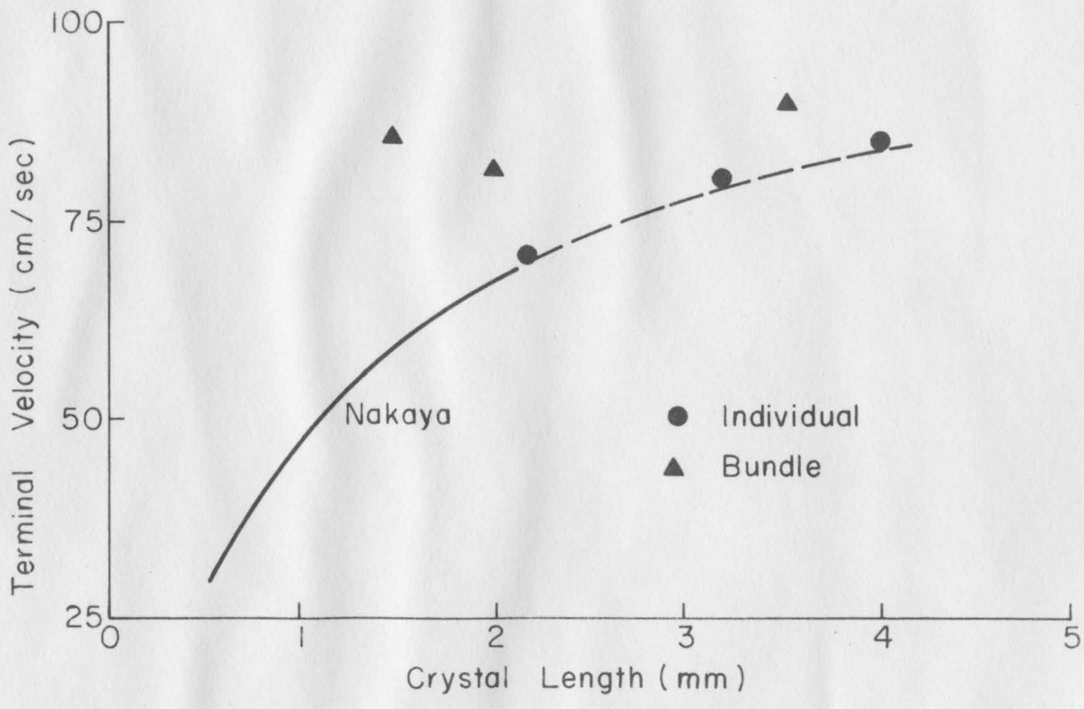

Figure 15. Relationship between terminal velocity and crystal length of needles and needle bundles

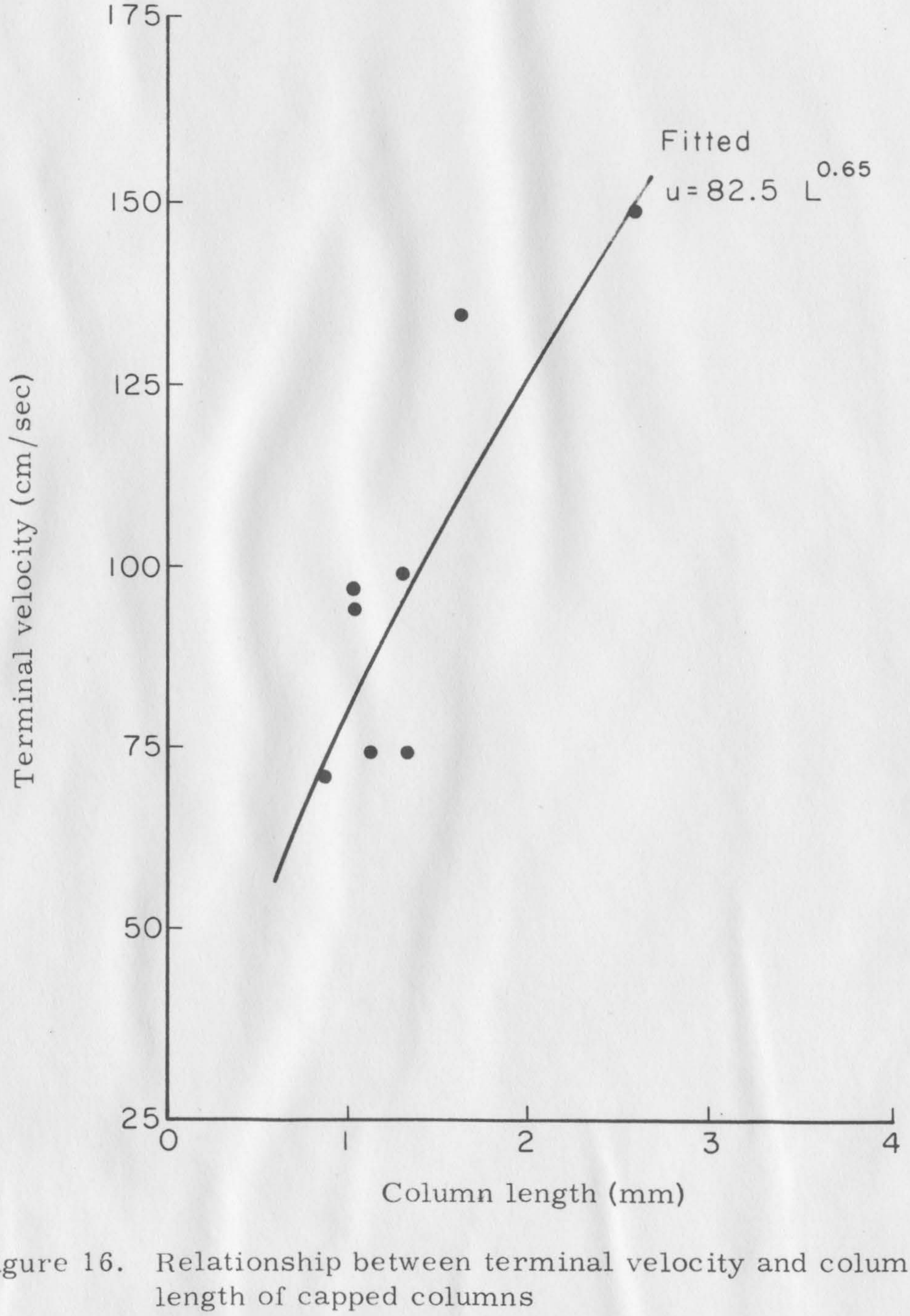

Figure 16. Relationship between terminal velocity and column length of capped columns

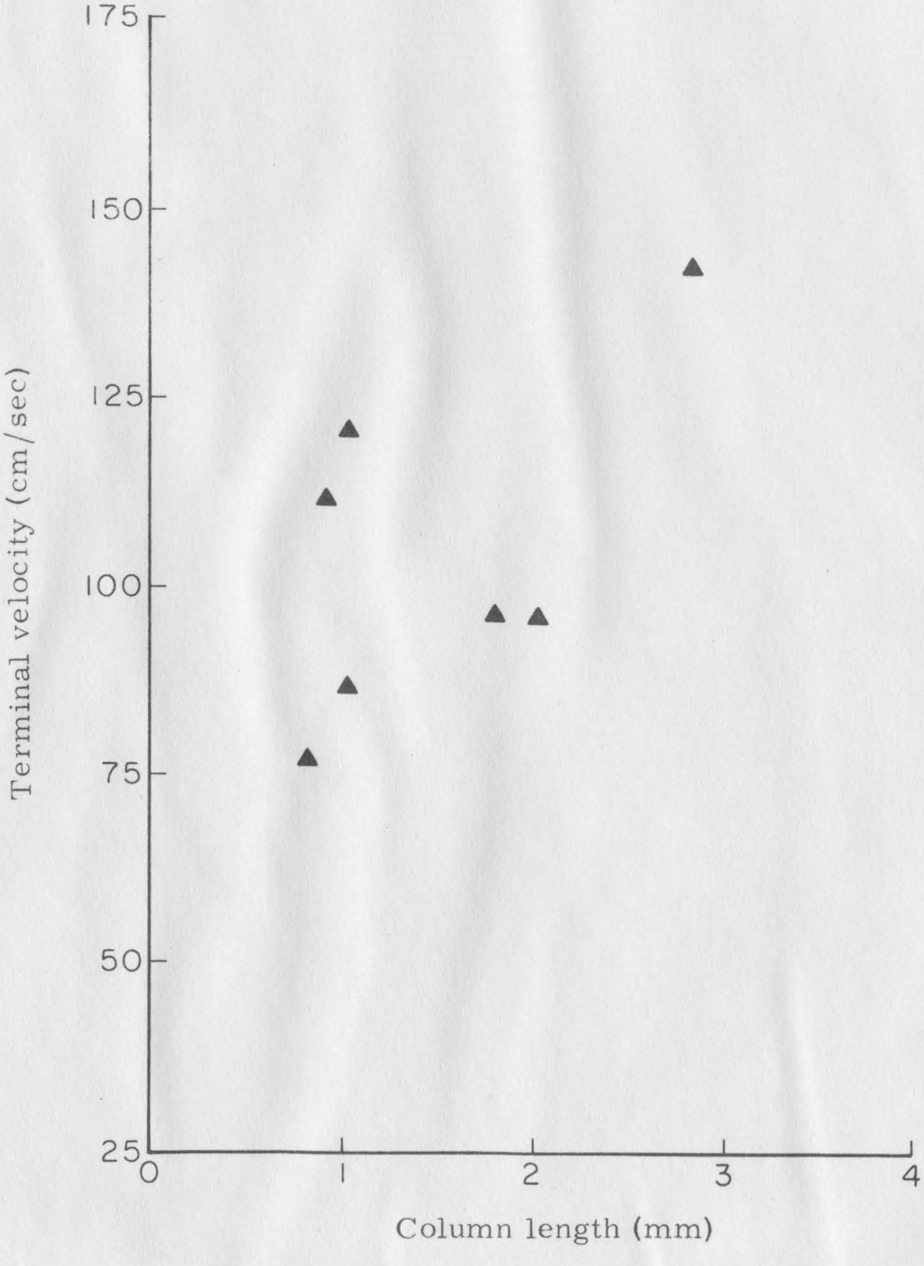

Figure 17. Relationship between terminal velocity and column length of multiple capped columns

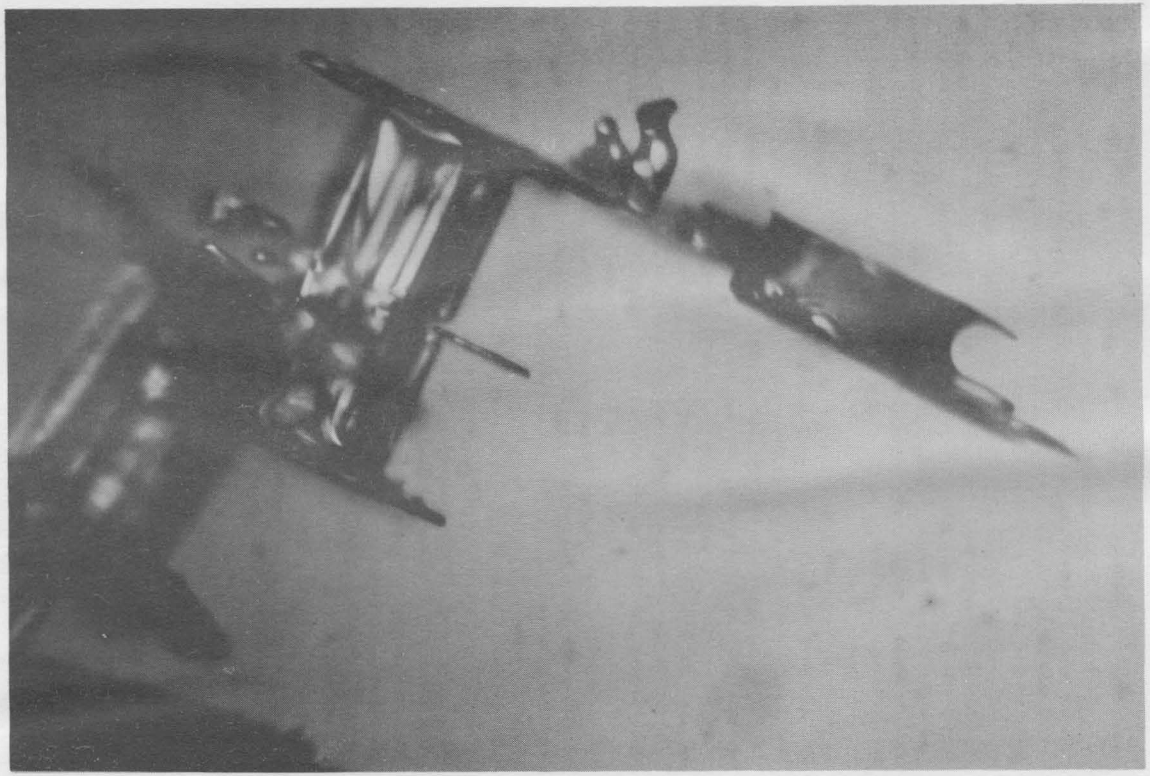

Figure 18. Example of multiple capped column encountered in study.

mass. It is evident from Fig. 16 that the experimental data tends to be compatible with this concept. Included in Fig. 16 is a curve which has been fitted to the data of the individual crystals.

A composite showing the fitted curves of the various crystal types is given in Fig. 1 . Also included are Nakaya's curves for comparison.

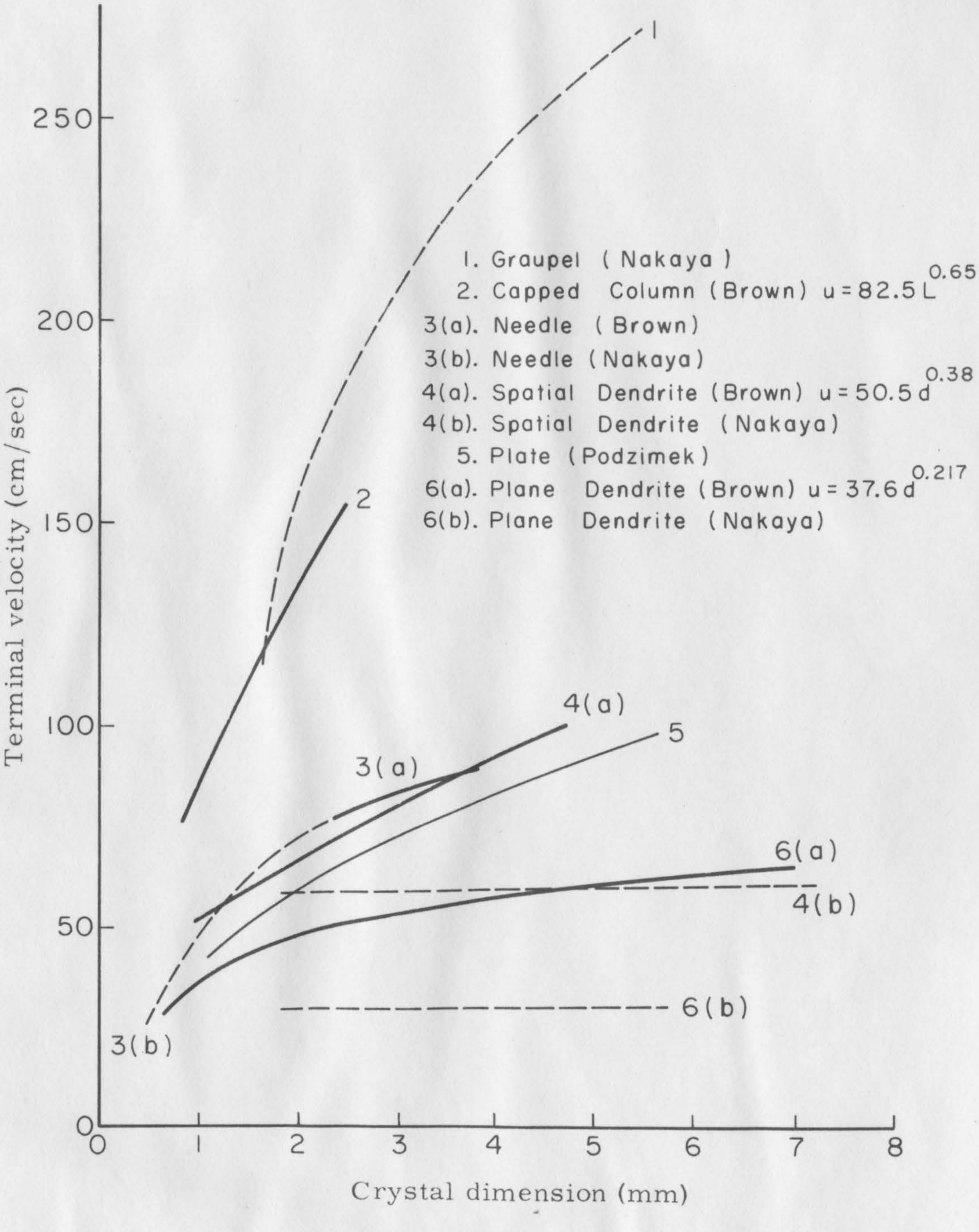

Figure 19. Composite showing curves which were fitted to data of various crystal types. Nakaya's curves are shown for comparison

SUMMARY

In this study, an attempt has been made to explain the terminal velocity-crystal size relationship from a theoretical aerodynamical standpoint for several crystal types. A parallel study has been carried out to measure the terminal velocities of ice crystals using a more refined technique than employed by Nakaya, and to establish values for the terminal velocities as a function of size for some of the crystal types not previously reported.

Experimental results of the study show that all of the crystal types observed exhibit a functional relationship between terminal velocity and crystal size in the size range considered. This is consistent with theoretical predictions developed in the study. Confidence in the method used is high because of its demonstrated repeatability and its improvements over the method used by Nakaya such as reduction of human error and the opportunity for recognizing particle acceleration.

The specific results of this study may be summarized as follows:

1. Theory predicts that the terminal velocity of plane dendrites should be greater than reported by Nakaya and in addition should show a functional relationship with crystal size, both diameter and thickness. This has been confirmed by the observations. The importance of crystal

thickness in controlling the terminal velocity was one result of the theoretical treatment. This parameter has been largely ignored in previous studies. A curve was fitted to the experimental data using the least squares technique and gave the relationship between terminal velocity and crystal diameter as: $U = 37.6\,d^{0.217}$.

2. Hexagonal plates were treated in the same manner as plane dendrites and a terminal velocity-crystal size curve was developed for them. Because plates have lower drag coefficients than plane dendrites, they have higher terminal velocities. Thus the plate curve is displaced towards higher velocities from the curve for plane dendrites. No natural plates were observed in the study for comparison with the theoretical treatment.

3. The volume and cross sectional area of a spatial dendrite can be determined by considering a sphere which just encloses the crystal. A certain fraction, x, of the sphere's volume would be ice. Similarly, if the crystal arms are projected on a cross section through the sphere, a fraction, y, of the cross sectional area would be ice. Theoretical considerations showed that the ratio x/y was one of the controlling factors in predicting terminal velocities. Observations showed in this study that natural crystals apparently do not maintain a constant x/y ratio

as they increase in size since the slope of the experimental data does not parallel theoretical curves. A curve fitted to the data is described by: $U = 50.5\,d^{0.38}$.

4. It was found from theoretical considerations that the terminal velocity of columns is dependent on the crystal radius and not directly on length. Jayaweera and Cottis (1969), using a similar theoretical approach, computed the terminal velocities of columns as a function of diameter and length/diameter ratio. Their results are included in this paper for comparison.

5. Needles are treated along with columns because of their similarity. They are classified as columns with much greater length than diameter by Jayaweera and Cottis (1969). The value of the length/diameter ratio at which the classification changes is not specified by them, however. Three natural needles were observed and their terminal velocity was plotted versus their length. Their terminal velocities could not be compared directly to the theoretical curves of Jayaweera and Cottis because the crystal diameters were greater than those included in their study. However, good agreement with Nakaya was found when his curve was extended to greater lengths.

6. Theoretical considerations predict that a capped column should behave like a thick plate of mass equal to that of

varies over the basin. C is the curve-fitting error introduced into the model parameters by a fitting process. The parameter values are perturbed from a global "best" set of values in order to minimize the fitting criterion, U, so that C is negative in sign. For use of the model in prediction, the curve fitting adds to the error, as indicated in table 2.

The fitted error criteria of set A for all three stations are quite similar to those for set B, although set A rainfall values are not adjusted to mean basin conditions. The bias in the recorded rainfall at each station was compensated for by the curve-fitting ability of the model to adjust parameter values. On the basis of these data, bias in amount of recorded rainfall affects the resulting fitted parameter values rather than the accuracy of fit. As the result of a change in value of the fit criterion of less than 1 percent, the parameter values from station 338 have changed so much that the parameter values for set B have a maximum of 1.36 for the ratio of highest to lowest value, the ratio for parameter EVC. For Set A five parameters had ratios greater than 1.36, PSP, RGF, BMSM, EVC, and DRN. The fitted parameter value for station 338 is one of the extreme values for each of those parameters in both set A and set B. Thus, the errors seem to be transferred from the data to the parameters, as is particularly evident for station 338.

Input set C contains variability among the three inputs only in the time distribution of rainfall. The goodness of fit for this set ranged from 0.100 for station 60 to 0.152 for station 338. Converting the range of 0.052 to an average percentage error for the peaks yields an estimate of about a 23 percent error in peak discharge reproduction introduced by time variability alone. Therefore for a basin with this degree of variation in rainfall patterns and the relative smoothing action introduced by the model and, hopefully, by the hydrology, an average error of as much as 20 percent for simulated flood peaks can be introduced by the time distribution error alone. Considering only the two "better" or seemingly more representative gages, the difference in fitted U1 values is, 0.017 which gives an average percentage error of 13 percent introduced by time distribution error in a "good" record.

In set C the most representative gage, judged in terms of goodness of fit, was that closest to the center of the basin. The least representative was on the perimeter and at the highest elevation of the basin. Therefore, relative representativeness was about as expected.

Input set B contains both time distribution erros within a storm and storm volume errors. The records have been adjusted to minimize only the station bias in relation to basin mean annual rainfall. The results of Set B runs indicate that station 447 probably is the most representative station for predicting storm volumes, just as results of set C runs indicate that station 60 probably is the most representative for time distribution of rainfall within a storm.

An estimate of the volume error component for station 60 should be about the sum of the differences between the values of the objective functions for the B and C runs for the two stations. Thus, volume errors can introduce as much as 0.04 to U1, which is on the order of 20 percent errors. The compounding of the time distribution errors of station 477 and the storm volume errors of station 60 would give a U1 of 0.057, which leads to a possible combined rainfall data error component on the order of a 24 percent standard error.

Effect of Screened Data

All data used in fitting was screened for gross flyers or outliers. The fitted parameters will predict within the indicated range of accuracy for other data which contain the same range of errors as in the screened data. The screened data used for fitting contain the usual range of errors normally encountered. However, grossly inadequate or unrepresentative data will produce outliers well beyond the errors of the indicated prediction. If data are grossly in error, modeling results using that erroneous data should be expected to be in error also.